ACS APPLIED MATERIALS & INTERFACES

Research Article

www.acsami.org

Synthesis of Amphiphilic Brookite Nanoparticles with High Photocatalytic Performance for Wide Range of Application

Ken-ichi Katsumata,*[,†] Yukiaki Ohno,[‡] Koji Tomita,[‡] Takaaki Taniguchi,[§] Nobuhiro Matsushita,[†] and Kiyoshi Okada[†]

[†]Materials and Structures Laboratory, Tokyo Institute of Technology, 4259 Nagatsuta, Midori, Yokohama, Kanagawa 226-8503, Japan

[‡]Department of Chemistry, School of Science, Tokai University, 1117 Kitakaname, Hiratsuka, Kanagawa 259-1292, Japan,

[§]Graduate School of Science and Technology, Kumamoto University, 2-39-1 Kurokami, Kumamoto, 860-8555, Japan

Supporting Information

ABSTRACT: Brookite TiO_2 nanoparticles with amphiphilic properties were successfully synthesized with a water-soluble titanium glycolate complex precursor using an oleate-modified hydrothermal growth process. The ~20−40 nm TiO_2 nanoparticles were highly dispersible in both water and cyclohexane. The activity of the brookite nanoparticles for the degradation of acetaldehyde under UV irradiation was higher than that of Degussa P-25 TiO_2 powder. A spin-coated brookite film prepared on a polyimide substrate exhibited photoinduced hydrophilicity. Thus, these synthesized brookite nanoparticles could be applied as a photocatalytic coating solution.

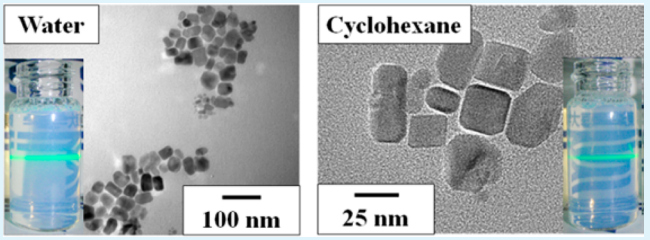

KEYWORDS: *brookite, hydrothermal method, oleic acid, amphiphilicity, photocatalyst, photoinduced hydrophilicity*

INTRODUCTION

Titanium dioxide (TiO_2) is an efficient photocatalyst that is activated by irradiation with ultraviolet (UV) light to generate electron-hole pairs, which reduce and oxidize adsorbates on a surface, thereby producing species such as OH radicals and O_2^-.[1−3] These radicals have strong oxidation activity and can decompose most organic compounds[4−12] and bacteria.[13−18] Therefore, many studies have been conducted on the application of TiO_2 to water[19−21] and air purification.[22−27]

The photoinduced hydrophilicity, as well as conventional applications, of the TiO_2 photocatalyst has been studied since 1995.[28−31] UV irradiation of TiO_2 generates a highly hydrophilic state on the surface.[32−40] If the surface is coated with an organic material, then the photocatalytic decomposition of organic compounds firstly regenerates a hydrophilic surface and then a highly hydrophilic surface by increasing the number of hydroxyl groups.[41,42] This unique property has already been applied to various industrial products, such as self-cleaning exterior tiles, anti-beading automobile side mirrors, and anti-fogging glasses.[2,43−46]

TiO_2 in nature as mainly three polymoophs; anatase (space group: $I4_1/amd$), rutile ($P4_2/mnm$), and brookite ($Pbca$). Rutile is the most stable phase, whereas the other two phases are metastable and transform to rutile when heated at high temperatures. The synthesis and applications of anatase and rutile have been extensively studied, because they are relatively easy to synthesize.[47−55] In contrast, brookite is a rare TiO_2 polymorph and is typically difficult to synthesize.

Recently, the synthesis of brookite nanoparticles with various morphologies, such as nanorods, nanotubes, and nanoflowers, has been reported.[56−65] Kominami et al.[56] reported the synthesis of nanosized brookite particles by a solvothermal method. Ohtani et al.[66] reported that brookite exhibited higher photocatalytic activity than anatase and rutile. Kandiel et al.[61] also reported that the activity of a pure brookite suspension for photocatalytic H_2 evolution was higher than that of pure anatase, despite the former having a lower specific surface area. In addition, Koelsch et al.[67] suggested that brookite is a good candidate for photovoltaic devices. However, these brookite particles were synthesized using Ti sources with strong toxicological and corrosive properties ($TiCl_3$, $TiCl_4$, and titanium alkoxides) that are difficult to handle.

It has been successfully synthesized highly anisotropic, one-dimensional shaped single-phase brookite nanoparticles using a water-soluble titanium complex precursor that was stable over a wide pH range and environmentally benign.[68−71] The nanoparticles had high crystallinity, but the morphology was not well controlled and was heavily agglomerated. It is considered that these synthesized brookite nanoparticles difficult to apply as a photocatalytic coating solution. We have succeeded in the synthesis of an aqueous dispersion of highly crystalline brookite nanoparticles with controlled morphology, using an oleate-

Received: June 29, 2012
Accepted: August 3, 2012
Published: August 3, 2012

modified growth technique.[72] However, the brookite nanoparticles were only dispersible in water.

In the present study, amphiphilic brookite nanoparticles were prepared using a water-soluble titanium complex and the oleate-modified hydrothermal growth process. The photocatalytic activity (photocatalytic oxidation activity and photoinduced hydrophilicity) of the particles was evaluated according to the photodegradation of acetaldehyde gas and the water contact angle.

EXPERIMENTAL SECTION

Materials. Titanium powder (Ti, −45 μm particle size, 99.9%), ammonia solution (NH_3, 28%), hydrogen peroxide (H_2O_2, 30%), sodium oleate ($C_{17}H_{33}COONa$, 60%), and cyclohexane (C_6H_{12}, 99.5%) were purchased from Wako Pure Chemical Industries, Tokyo, Japan. Glycolic acid ($HOCH_2COOH$, 97%) was purchased from Kanto Chemicals Co. Inc., Tokyo, Japan. Water was purified using a Millipore installation.

Synthesis of Brookite Nanoparticles. The synthesis of brookite nanoparticles has been previously described in detail.[72] Titanium powder (2.0 mmol) was dissolved in a cooled 28% NH_3 aqueous solution (2.0 mL) containing 30% H_2O_2 (8.0 mL). After stirring for 2 h, the titanium powder was completely dissolved, and glycolic acid (3.0 mmol) was then added to the solution as a complexant agent. The solution was dried at 65°C to remove excess H_2O_2 and NH_3. The gel was dissolved by the addition of distilled water to yield a transparent yellow aqueous solution. The initial pH of the glycolate titanium complex solution was approximately 6. Various amounts of sodium oleate (1.0, 2.0, and 4.0 mmol) dissolved in distilled water (18 mL) were added to the solution containing glycolate titanium complex ions. The total volume of the solution was adjusted to 20 mL using distilled water, which resulted in a pH of 8. The solution was sealed in a Teflon-lined stainless steel autoclave (50 mL) and heated at 200°C for 6 h. After the hydrothermal reaction, the white precipitate formed was separated from the solution by centrifugation (6000 rpm for 30 min), and was then washed several times with distilled water.

Preparation of Brookite Films. Brookite film was produced by spin coating a 0.1 M cyclohexane solution of brookite nanoparticles onto a polyimide substrate at 2000 rpm for 30 s in dry air. After coating, the film was dried at 80°C for 6 h. In the case of a glass substrate, brookite film was produced by spin coating a 0.1 M water solution of brookite nanoparticles at 2000 rpm for 30 s in dry air. After coating, the film was fired at 350°C for 1 h.

Characterization. The crystalline phase of the samples was identified by powder X-ray diffraction (XRD; RINT2100, Rigaku, Japan) with monochromated Cu Kα radiation. The applied voltage and current to the Cu target was 40 kV and 40 mA, respectively. The particle size and morphology of the samples were investigated by transmission electron microscopy (TEM; HF-2000, Hitachi, Japan) with operation at 200 kV. TEM samples were prepared by depositing one drop of the sample dispersed in cyclohexane or water onto an amorphous carbon grid. The zeta potentials of the samples were measured by laser Doppler microelectrophoresis (Zetasizer Nano ZS, Malvern Instruments Ltd., UK). The samples were suspended in distilled water and the pH was adjusted using HCl or NaOH solution. Fourier transform infrared spectroscopy (FT-IR) was performed using a JIR-7000, JEOL, Japan. The specific surface area of the samples was estimated by the Brunauer, Emmett, Teller (BET) method using an adsorption instrument (ASAP2010, Shimadzu Co., Japan).

Evaluation of Photocatalytic Activity. The degradation of gaseous acetaldehyde (CH_3CHO) by brookite powder samples was conducted in a batch-type reactor at room temperature, which is higher than the boiling point of pure acetaldehyde (approximate 20°C). The 500 mL reactor vessel was made of Pyrex glass. The samples were irradiated in air using UV light (1.0 mW/cm^2) for 2 days before photodegradation to remove ubiquitous organic pollutants or oleate molecules on the surface. The brookite powder samples (0.05 g) were placed in the reaction vessel and a measured quantity of acetaldehyde gas (8.9 μmol, 400 ppm) was introduced into the reaction vessel using a Pressure-Lok precision analytical syringe. After adsorption equilibration in the dark for 1 h, the reactor was placed beneath black-light lamps (Toshiba, FL10BLB, wavelength range of 290−420 nm with a peak at 352 nm). The UV light intensity was 1.0 mW/cm^2 as measured with a UV radiometer (UVR-400, Iuchi, Japan). The decrease in acetaldehyde concentration and increase in CO_2 concentration were monitored by gas chromatography with nitrogen as the carrier gas (GC-14A, Shimadzu, 2 m Porapak-Q column ZP-17 and flame ionization detector). The photoinduced hydrophilicity of the film sample surfaces was evaluated according to the water contact angle (θ), which was measured using a commercial automatic contact angle meter (DMs-400, Kyowa Interfaces Science, Japan). The water droplet volume used for the measurements was 3.0 μL. The average of three separate measurements was taken as the water contact angle.

RESULTS AND DISCUSSION

Figure 1 shows XRD patterns of samples synthesized by the hydrothermal treatment at 200°C for 6 h with various amounts of sodium oleate additive. All reflections in the XRD patterns of the sample prepared with 2.0 mmol of sodium oleate can be assigned to the brookite phase. In contrast, both brookite and anatase crystalline phases were detected in the samples prepared with 1.0 and 4.0 mmol of sodium oleate. No reflections assignable to the rutile TiO_2 phase were observed in the XRD patterns. However, only the rutile phase was obtained without sodium oleate addition.[68] These results indicate that the brookite phase is formed with increasing Na^+ ion concentration during the hydrothermal treatment. It has been reported that the presence and concentration of Na^+ ions are important factors to obtain the brookite phase.[73−77] Zhao et al.[60] reported that anatase phase is obtained with low Na^+ ion concentration, which corresponds with the result shown in Figure 1a. Kominami et al.[56,78] reported that the presence of alkaline or alkaline earth metals and the ratio of titanium to the alkaline or alkaline earth metals are important for the formation of brookite. Kobayashi et al.[79] also reported that a weakly basic environmental condition promotes the formation of brookite. Thus, a weakly basic condition (pH 8) and 2.0 mmol of sodium

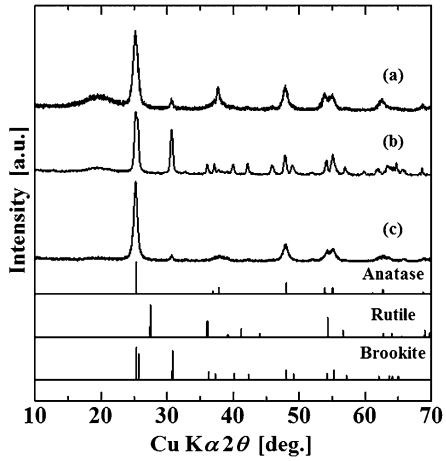

Figure 1. XRD patterns of the samples synthesized by the hydrothermal treatment at 200 °C for 6 h with various amounts of sodium oleate additive; (a) 1.0, (b) 2.0, and (c) 4.0 mmol. The standard patterns for anatase (ICDD#00-021-1272), rutile (ICDD#00-021-1276), and brookite (ICDD#00-029-1360) are shown at the bottom for reference.

dx.doi.org/10.1021/am301183t | ACS Appl. Mater. Interfaces 2012, 4, 4846−4852

oleate additive are considered to be the optimum conditions to obtain the brookite phase.

Samples synthesized by the hydrothermal treatment using 2.0 mmol of sodium oleate were redispersed in water or cyclohexane, to form transparent colloidal solutions, as shown in Figure 2. The Tyndall phenomenon was confirmed in both

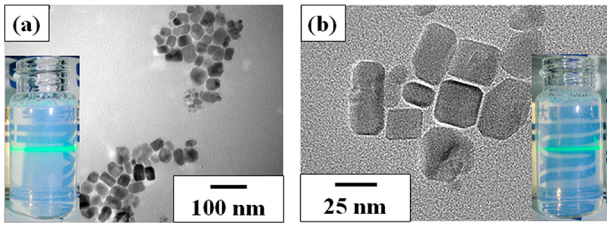

Figure 2. TEM images of the brookite nanoparticles dispersed in (a) water and (b) cyclohexane, synthesizing by the hydrothermal treatment at 200 °C for 6 h with 2.0 mmol of sodium oleate. Inset photographs show that the synthesized nanoparticles exhibit excellent dispersibility in both solutions.

solutions by the visibility of a green laser path, which indicates the high dispersibility of the synthesized brookite particles. In addition, the brookite particles are dispersible in both polar (water) and non-polar (cyclohexane) solvents, i.e., the brookite particles are amphiphilic. This is distinctly different from brookite powder synthesized without sodium oleate. Images a and b in Figure 2 shows TEM images of the brookite nanoparticles dispersed in water and cyclohexane, respectively. The brookite nanoparticles in both solutions exhibit excellent two-dimensional dispersibility on the amorphous carbon grid.

The morphology of the brookite nanoparticles was squarish without sharp angles and the particle size was 20−40 nm, which is in good agreement with our previous report.[72] The effect of sodium oleate addition on the shape of anatase particles has been investigated,[80] where sharp-edged cubic anatase particles were obtained. Sodium oleate may specifically adsorb onto the {001} and {100} facets, which would significantly reduce the specific surface energy and induce the formation of the cubic shape. It is considered that the squarish morphology of the brookite nanoparticles is achieved by the selective adsorption of oleate molecules onto the {001} and {210} facets of brookite, which lowers the surface energy, because the brookite nanoparticles synthesized with oleate are surrounded by four {001} and two {210} facets.[72]

Figure 3 shows the effect of oleate addition on the zeta potentials of brookite nanoparticle surfaces. The zeta potentials at pH 6 and 8 (under near-neutral pH conditions) were −50.6 and −55.2 mV, respectively. In contrast, the zeta potentials of brookite nanoparticles synthesized without oleate were -24.6 mV (pH 6) and −31.4 mV (pH 8) (see Figure S1 in the Supporting Information). Thus, the zeta potentials of both samples synthesized with oleate became more negative and were lower than those synthesized without oleate. The negative charge of the nanoparticles is generally attributed to hydroxyl groups (OH^-) on the nanoparticle surfaces. Fourier transform-infrared (FT-IR) spectral measurements of brookite nanoparticles synthesized with and without oleate indicated no significant difference in the adsorption of hydroxyl groups (OH^-) (see Figure S2 in the Supporting Information). We have suggested an oleate double layer model for the nanoparticle surfaces.[81] Models for the oleate layers formed on the brookite (001) and (210) facets in water are shown in

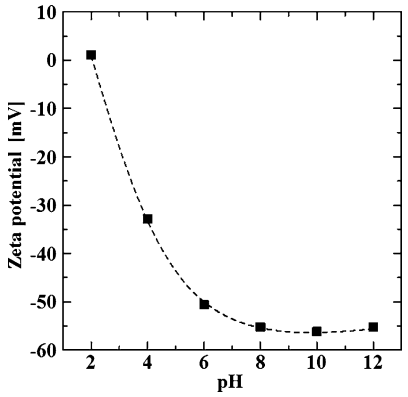

Figure 3. Zeta potentials of the synthesized brookite nanoparticle surfaces at various pHs.

Scheme 1a. The primary layer is formed by chemical bonding of the oleate carboxyl group onto surface active sites, which are Ti^{4+} or non-covalent bonding oxygen atoms, of the brookite (001) and (210) facets, and the secondary layer is formed by hydrophobic interactions among the alkyl chains of the oleate. Tombácz et al.[82] reported a large negative shift in the zeta potential by formation of the secondary oleate layer, which supports our proposed model.

Figure 4 shows the atomic arrangements of the ideal brookite TiO_2 (001) and (210) facets. The bonding between Ti and noncovalent bonding oxygen atoms in the outmost TiO_6 octahedra on the brookite (001) facet are inclined with respect to the [001] direction. In the case of the brookite (210) facet, they are slightly inclined with respect to the [210] direction. Considering that oleate molecules adsorb on the surface active sites (Ti^{4+} or noncovalent bonding oxygen atoms), oleate molecules are more randomly absorbed on the (001) facet than on the (210) facet. Thus, if oleate molecules in the primary layer absorb randomly on the (001) facet in water, then the molecules in the secondary layer would also be located randomly between molecules of the primary layer. In contrast, the arrangement of oleate molecules in the primary and secondary layers on the (210) facet in water is more order that on the (001) facets. (Scheme 1a) In the case of cyclohexane, the (001) and (210) facets are covered by only a primary layer. (Scheme 1b) Generally, the surface on the particles has electrostatic charge in a polar solvent except in the case of an isoelectric point, and the particles are dispersible in a polar solvent due to an electrostatic repulsion on the particle surface. In contrast, the particles are dispersible in a non-polar solvent due to not the electrostatic repulsion but the effect of steric hindrance by surfactants deposited on the particle surface. Thus, the brookite nanoparticles synthesized with oleate are dispersed by the effects of electrostatic stabilization and steric hindrance in water and cyclohexane, respectively.

Figure 5 shows the results of acetaldehyde (CH_3CHO) decomposition in the presence of the synthesized brookite nanoparticles and Degussa P-25 under UV light irradiation. The degradation of acetaldehyde and generation of CO_2 was similar for both samples. When UV light was irradiated onto a sample, the acetaldehyde concentrations began to decrease significantly, accompanied by CO_2 generation. After UV irradiation for 20 min, the acetaldehyde was completely degraded. CO_2 was gradually generated with increasing UV irradiation time. The oxidative photodegradation of acetaldehyde with a TiO_2 photocatalyst proceeds as follows[83]

Scheme 1. Oleate Layer Models Formed on Brookite (001) and (210) Facets in Water and Cyclohexane

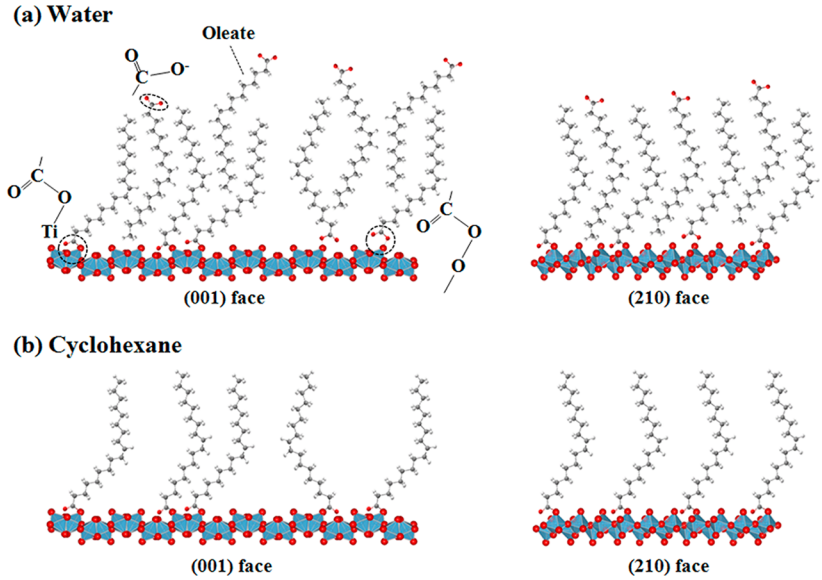

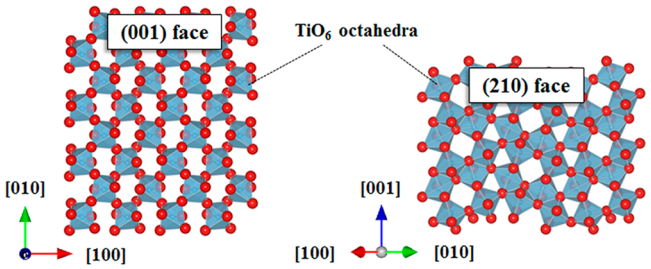

Figure 4. Schematic illustration of the ideal brookite TiO_2 (001) and (210) facet structures.

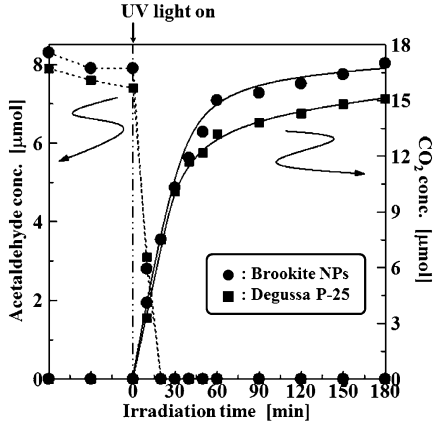

Figure 5. Change in acetaldehyde (dotted line) and CO_2 (solid line) concentrations as a function of irradiation time in the presence of synthesized brookite nanoparticles (●) and Degussa P-25 TiO_2 powder (■).

$$CH_3CHO(ads) + 3H_2O + 10h^+ \rightarrow 2CO_2 + 10H^+ \quad (1)$$

$$CH_3CHO(ads) + H_2O + 2h^+ \rightarrow CH_3COOH(ads) + 2H^+ \quad (2)$$

$$CH_3COOH(ads) + 2H_2O + 8h^+ \rightarrow 2CO_2 + 8H^+ \quad (3)$$

where h^+ is a hole generated by the photoinduced charge separation in TiO_2. One acetaldehyde molecule decomposes into two CO_2 molecules, which is the final product. The initial concentration of acetaldehyde gas introduced into the reaction vessel was 8.9 μmol, which would theoretically provide 17.8 μmol of CO_2. The CO_2 generation between the two samples is quite similar until 30 min, after which the CO_2 generation rate became different. The CO_2 generation rate of the brookite nanoparticles was higher than that of Degussa P-25, which was saturated at around 15 μmol. The CO_2 generation for the synthesized brookite nanoparticles was around 17 μmol after 180 min, which indicated that acetaldehyde was almost completely decomposed. Thus, the brookite nanoparticles exhibited higher activity for the photodecomposition of acetaldehyde than the Degussa P-25 powder.

The photocatalytic activity of TiO_2 is dependent on factors such as specific surface area (particle size), particle shape, crystallinity, and crystal phase. The specific surface area of the brookite nanoparticles (60 m^2/g) was slightly larger than that of the Degussa P-25 powder (50 m^2/g). Morishima et al.[69] reported that brookite nanoparticles synthesized by hydrothermal method using a water-soluble Ti-complex coordinated by ethylenediaminetetraacetic acid had higher specific surface area than P-25 powder, and the synthesized brookite nanoparticles exhibited photocatalytic activity higher than P-25. It has been reported that anatase TiO_2 (100) and (001) facets exhibit high photocatalytic activity, and it is suggested that the crystal arrangement of the anatase (100) and (001) facets contributes significantly to the photocatalytic activity.[84−86] Figure 6 shows the atomic arrangements for the anatase TiO_2 (100) and (001) facets, and the brookite TiO_2 (001) and (210) facets. For the anatase (100) and brookite (001) facets, there are non-covalent bonding oxygens and bridging oxygens. The non-covalent bonding oxygen is the termination on the anatase (100) and brookite (210) facets. The brookite (001) and (210) facets have atomic arrangements that are analogous to the anatase (100) and (001) facets, respectively. We consider that the synthesized brookite nanoparticles exhibit excellent activity for photodegradation of acetaldehyde.

dx.doi.org/10.1021/am301183t | ACS Appl. Mater. Interfaces 2012, 4, 4846−4852

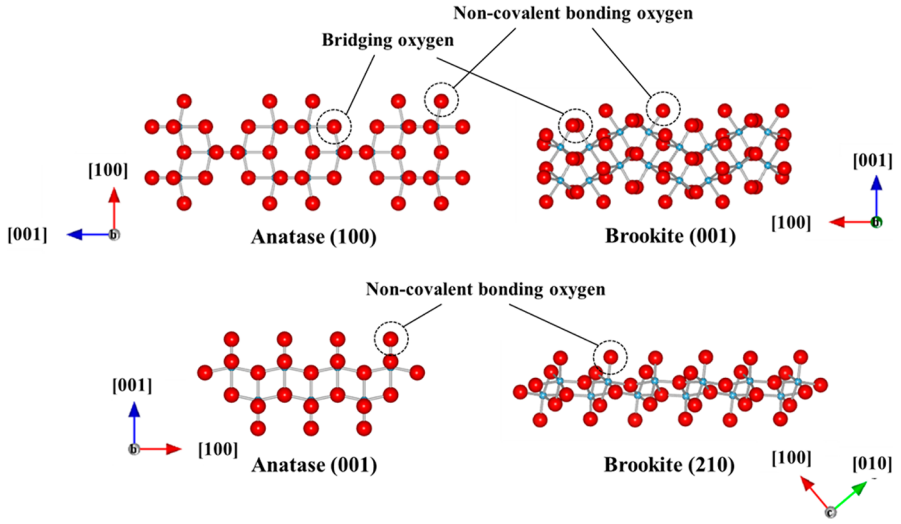

Figure 6. Atomic arrangements of the ideal anatase TiO_2 (100) and (001) facets, and brookite TiO_2 (001) and (210) facets.

Figure 7 shows the variation of the water contact angle for a brookite film and polyimide substrate (blank sample) as a function of UV irradiation time. The initial contact angle of the film was quite high, which may be due to the oleate on the brookite nanoparticle surfaces. When UV light was irradiated on the film, the contact angle increased, and then began to decrease. It is considered that the hydrophilic conversion started after decomposition of the oleate on the brookite nanoparticles by photocatalytic reaction. The contact angle of the film became less than 3° after irradiation for 150 min, which corresponds to a highly hydrophilic state. In contrast, the contact angle of the blank sample did not decrease with increasing UV irradiation time, which indicates that the brookite film exhibits photoinduced hydrophilicity under UV irradiation.

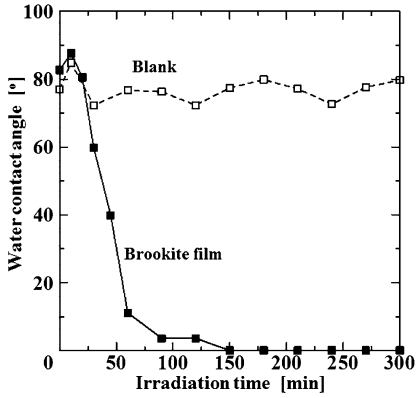

Figure 7. Variation of water contact angle on a brookite film and polyimide substrate (blank) under UV irradiation (1.0 mW/cm^2) over time.

Brookite film could be prepared on an organic substrate using brookite nanoparticles dispersed in cyclohexane solvent. The film had good transparency and the film surface was dense (see Figures S3 and S4 in the Supporting Information). Brookite film could also be prepared on an inorganic substrate (glass) using water as a solvent, and the quality of the film was the same as that prepared on the organic substrate. It is considered that the results of this work will be useful to widen the applications of the brookite nanoparticles.

CONCLUSIONS

Brookite TiO_2 nanoparticles were synthesized from a glycolate titanium complex precursor using an oleate-modified hydrothermal method (200 °C, 6 h). The crystal phase was dependent on the amount of oleate additive. Single phase brookite was produced when the amount of additive was 2 mmol (Ti/oleate = 1.0 molar ratio), where the anatase phase was also obtained at other Ti/oleate molar ratios. The morphology of the brookite nanoparticles was squarish, and the nanoparticles were amphiphilic, in that they were dispersible in both water and cyclohexane. It is thought that the brookite nanoparticle surfaces were modified by an oleate double layer. The brookite nanoparticles and a spin-coated brookite film exhibited high activity for the photodegradation of acetaldehyde and excellent hydrophilic conversion under UV irradiation, respectively. The present method is considered to be very effective for the synthesis of amphiphilic nanoparticles, and could be applicable to the synthesis of other metal oxides.

ASSOCIATED CONTENT

Supporting Information

Zeta potential measurements and FT-IR spectra of samples synthesized by the hydrothermal method. SEM image and photograph of the brookite film prepared on an organic substrate using the brookite nanoparticles dispersed in cyclohexane. This Information is available free of charge via the Internet at http://pubs.acs.org/.

AUTHOR INFORMATION

Corresponding Author

*Tel: +81-45-924-5323. Fax: +81-45-924-5358. E-mail: katsumata.k.ab@m.titech.ac.jp.

Notes

The authors declare no competing financial interest.

ACKNOWLEDGMENTS

The authors are grateful to Mr. Y. Komatsubara (Tokyo Institute of Technology, Japan) for his assistance with the TEM observation and Prof. Y. Kitamoto (Tokyo Institute of Technology, Japan) for the TEM. The authors are grateful to Prof. T. Akatsu for the XRD. The authors are also grateful to Dr. K. Momma and Dr. F. Izumi (National Institute for

Materials Science, Japan) for the VESTA program. This research was partially supported by a Grant-in-Aid for Young Scientists (B, 23750238) from the Ministry of Education, Culture, Sports, Science, and Technology of Japan.

REFERENCES

(1) Fujishima, A.; Honda, K. *Nature* **1972**, *238*, 37−38.
(2) Fujishima, A.; Rao, T.N.; Tryk, D.A. *J. Photochem. Photobiol. C: Photochem. Rev.* **2000**, *1*, 1−21.
(3) Fujishima, A.; Zhang, X. *C. R. Chim.* **2006**, *9*, 750−760.
(4) Kawai, T.; Sakata, T. *Nature* **1980**, *286*, 474−476.
(5) Ohko, Y.; Tryk, D.A.; Hashimoto, K.; Fujishima, A. *J. Phys. Chem. B* **1998**, *102*, 2699−2704.
(6) Sawunyama, P.; Fujishima, A.; Hashimoto, K. *Langmuir* **1999**, *15*, 3551−3556.
(7) Nakamura, I.; Negishi, N.; Katsuna, S.; Ihara, T.; Sugihara, S.; Takeuchi, K. *J. Mol. Catal. A: Chem.* **2000**, *161*, 205−212.
(8) Ikeda, S.; Sugiyama, N.; Murakimi, S.; Kominami, H.; Kera, Y.; Noguchi, H.; Uosaki, K.; Torimoto, T.; Ohtani, B. *Phys. Chem. Chem. Phys.* **2003**, *5*, 778−783.
(9) López, M. C.; Fernández, M. I.; Rodríguez, S.; Santaballa, J. A.; Steenken, S.; Vulliet, E. *ChemPhysChem* **2005**, *6*, 2064−2074.
(10) Tachikawa, T.; Majima, T. S *Langmuir* **2009**, *25*, 7791−7802.
(11) D'Arienzo, M.; Crippa, M.; Essawy, A. A.; Scotti, R.; Wahba, L.; Morazzoni, F.; Gentile, P.; Bellobono, I. R.; Polozzi, S. *J. Phys. Chem. C* **2010**, *114*, 15755−15762.
(12) Henderson, M. A.; Deskins, N. A.; Zehr, R. T.; Dupuis, M. *J. Catal.* **2011**, *279*, 205−212.
(13) Sunada, K.; Kukuchi, Y.; Hashimoto, K.; Fujishima, A. *Environ. Sci. Technol.* **1998**, *32*, 726−728.
(14) Sunada, K.; Watanabe, T.; Hashimoto, K. *Environ. Sci. Technol.* **2003**, *37*, 4785−4789.
(15) Sunada, K.; Watanabe, T.; Hashimoto, K. *J. Photochem. Photobiol. A: Chem.* **2003**, *156*, 227−233.
(16) Vohra, A.; Goswami, D. Y.; Deshpande, D. A.; Block, S. S. *J. Ind. Microbiol. Biotechnol.* **2005**, *32*, 364−370.
(17) Yeung, K. L.; Leung, W. K.; Yao, N.; Cao, S. *Catal. Today* **2009**, *143*, 218−224.
(18) Huang, H.; Leung, D. Y. C.; Li, G.; Leung, M. K. H.; Fu, X. *Catal. Today* **2011**, *175*, 310−315.
(19) Chen, J.; Liu, M.; Zhang, L.; Zhang, J.; Jin, L. *Water Res.* **2003**, *37*, 3815−3820.
(20) Zhang, D.; Li, G.; Yu, J. C. *J. Mater. Chem.* **2010**, *20*, 4529−4536.
(21) Schwitzgebel, J.; Ekerdt, J. G.; Gerischer, H.; Heller. *J. Phys. Chem.* **1995**, *99*, 5633−5638.
(22) Kolinko, P. A.; Kozlov, D. V.; Vorontsov, A. V.; Preis, S. V. *Catal. Today* **2007**, *122*, 178−185.
(23) Zhang, L.; Anderson, W. A.; Sawell, S.; Moralejo, C. *Chemosphere* **2007**, *68*, 546−553.
(24) Hodgson, A. T.; Destaillats, H.; Sullivan, D. P.; Fisk, W. J. *Indoor Air* **2007**, *17*, 305−316.
(25) Auvinen, J.; Wirtanen, L. *Atmos. Environ.* **2008**, *42*, 4101−4112.
(26) Zorn, M. E.; Hay, S. O.; Anderson, M. A. *Appl. Catal. B* **2010**, *99*, 420−427.
(27) Sekiguchi, K.; Morinaga, W.; Sakamoto, K.; Tamura, H.; Yasui, F.; Mehrjouei, M.; Müller, S.; Möller, D. *Appl. Catal. B* **2010**, *97*, 190−197.
(28) Wang, R.; Hashimoto, K.; Fujishima, A.; Chikuni, M.; Kojima, E.; Kitamura, A.; Shimohigoshi, M.; Watanabe, T. *Nature* **1997**, *388*, 431−432.
(29) Wang, R.; Hashimoto, K.; Fujishima, A.; Chikuni, M.; Kojima, E.; Kitamura, A.; Shimohigoshi, M.; Watanabe, T. *Adv. Mater.* **1998**, *10*, 135−138.
(30) Wang, R.; Sakai, N.; Fujishima, A.; Watanabe, T.; Hashimoto, K. *J. Phys. Chem. B* **1999**, *103*, 2188−2194.
(31) Watanabe, T.; Nakajima, A.; Wang, R.; Minabe, M.; Koizumi, S.; Fujishima, A.; Hashimoto, K. *Thin Solid Films* **1999**, *351*, 260−263.
(32) Nakajima, A.; Koizumi, S.; Watanabe, T.; Hashimoto, K. *Langmuir* **2000**, *16*, 7048−7050.
(33) Shibata, T.; Irie, H.; Ohmori, M.; Nakajima, A.; Watanabe, T.; Hashimoto, K. *Phys. Chem. Chem. Phys.* **2004**, *6*, 1359−1362.
(34) Katsumata, K.; Nakajima, A.; Yoshikawa, H.; Shiota, T.; Yoshida, N.; Watanabe, T.; Kameshima, Y.; Okada, K. *Surf. Sci.* **2005**, *579*, 123−130.
(35) Takeuchi, M.; Sakamoto, K.; Martra, G.; Coluccia, S.; Anpo, M. *J. Phys. Chem. B* **2005**, *109*, 15422−15428.
(36) Katsumata, K.; Nakajima, A.; Yoshida, N.; Watanabe, T.; Kameshima, Y.; Okada, K. *Surf. Sci.* **2005**, *596*, 197−205.
(37) Irie, H.; Washizuka, S.; Watanabe, Y.; Kako, T.; Hashimoto, K. *J. Electrochem. Soc.* **2005**, *152*, E351−E356.
(38) Katsumata, K.; Nakajima, A.; Shiota, T.; Yoshida, N.; Watanabe, T.; Kameshima, Y.; Okada, K. *J. Photochem. Photobiol. A: Chem.* **2006**, *180*, 75−79.
(39) Yan, X.; Abe, R.; Ohno, T.; Toyofuku, M.; Ohtani, B. *Thin Solid Films* **2008**, *516*, 5872−5876.
(40) Katsumata, K.; Ohno, Y.; Tomita, K.; Sakai, M.; Nakajima, A.; Kakihana, M.; Fujishima, A.; Matsushita, N.; Okada, K. *Photochem. Photobiol.* **2011**, *87*, 988−994.
(41) Sakai, N.; Fujishima, A.; Watanabe, T.; Hashimoto, K. *J. Phys. Chem. B* **2001**, *105*, 3023−3026.
(42) Sakai, N.; Fujishima, A.; Watanabe, T.; Hashimoto, K. *J. Phys. Chem. B* **2003**, *107*, 1028−1035.
(43) Fujishima, A.; Hashimoto, K.;Watanabe, T. *TiO_2 Photocatalyst, Fundamentals and Applications*; BKC Inc.: Tokyo, 1999.
(44) Carp, O.; Huisman, C. L.; Reller, A. *Prog. Solid State Chem.* **2004**, *32*, 33−177.
(45) Hashimoto, K.; Irie, H.; Fujishima, A. *Jpn. J. Appl. Phys.* **2005**, *44*, 8269−8285.
(46) Fujishima, A.; Zhang, X.; Tryk, D. A. *Surf. Sci. Rep.* **2008**, *63*, 515−582.
(47) Zhang, D.; Yoshida, T.; Oekermann, T.; Furuta, K.; Minoura, H. *Adv. Funct. Mater.* **2006**, *16*, 1228−1234.
(48) Bavykin, D. V.; Friedrich, J. M.; Walsh, F. C. *Adv. Mater.* **2006**, *18*, 2807−2824.
(49) Cozzoli, P. D.; Curri, M. L.; Giannini, C.; Agostiano, A. *Small* **2006**, *2*, 413−421.
(50) Fisher, A.; Kuemmel, M.; Jarn, M.; Linden, M.; Boissiere, C.; Nicole, L.; Sanchez, C.; Grosso, D. *Small* **2006**, *2*, 569−574.
(51) Hu, Y. S.; Kienle, L.; Guo, Y. G.; Maier, J. *Adv. Mater.* **2006**, *18*, 1421−1426.
(52) Wang, K.; Wei, M.; Morris, M. A.; Zhou, H.; Holmes, J. D. *Adv. Mater.* **2007**, *19*, 3016−3020.
(53) Chen, K. S.; Liu, W. H.; Wang, Y. H.; Lai, C. H.; Chou, P. T.; Lee, G. H.; Chen, K.; Chen, H. Y.; Chi, Y.; Tung, F. C. *Adv. Funct. Mater.* **2007**, *17*, 2964−2974.
(54) Zhou, Z.; Shinar, R.; Allison, A. J.; Shinar, J. *Adv. Funct. Mater.* **2007**, *17*, 3530−3537.
(55) Liu, Z. Y.; Sun, D. D.; Guo, P.; Leckie, J. O. *Chem.—Eur. J.* **2007**, *13*, 1851−1855.
(56) Kominami, H.; Kohno, M.; Kera, Y. *J. Mater. Chem.* **2000**, *10*, 1151−1156.
(57) Pottier, A.; Chanéac, C.; Tronc, E.; Mazerolles, L.; Jolivet, J. P. *J. Mater. Chem.* **2001**, *11*, 1116−1121.
(58) Bakardjieva, S.; Stengl, V.; Szatmary, L.; Subrt, J.; Lukac, J.; Murafa, N.; Niznansky, D.; Cizek, K.; Jirkovsky, J.; Petrova, N. *J. Mater. Chem.* **2006**, *16*, 1709−1716.
(59) Lee, B. I.; Wang, X.; Bhave, R.; Hu, M. *Mater. Lett.* **2006**, *60*, 1179−1183.
(60) Zhao, B.; Chen, F.; Huang, Q.; Zhang, J. *Chem. Commun.* **2009**, *34*, 5115−5117.
(61) Kandiel, T. A.; Feldhoff, A.; Robben, L.; Dillert, R.; Bahnemann, D. W. *Chem. Mater.* **2010**, *22*, 2050−2060.
(62) Deng, Q.; Wei, M.; Ding, X.; Jiang, L.; Ye, B.; Wei, K. *Chem. Commun.* **2008**, *31*, 3657−3659.

(63) Buonsanti, R.; Snoeck, E.; Giannini, C.; Gozzo, F.; Garcia-Hernandez, M.; Garcia, M. A.; Cingolani, R.; Cozzoli, P. D. *Phys. Chem. Chem. Phys.* **2009**, *11*, 3680−3691.
(64) Buonsanti, R.; Grillo, V.; Carlino, E.; Giannini, C.; Kipp, T.; Cingolani, R.; Cozzoli, P. D. *J. Am. Chem. Soc.* **2008**, *130*, 11223−11233.
(65) Buonsanti, R.; Grillo, V.; Carlino, E.; Giannini, C.; Gozzo, F.; Garcia-Hernandez, M.; Garcia, M. A.; Cingolani, R.; Cozzoli, P. D. *J. Am. Chem. Soc.* **2010**, *132*, 2437−2464.
(66) Ohtani, B.; Handa, J.; Nishimoto, S.; Kagiya, T. *Chem. Phys. Lett.* **1985**, *120*, 292−294.
(67) Koelsch, M.; Cassaignon, S.; Guillemoles, J. F.; Jolivet, J. R. *Thin Solid Films* **2002**, *403-404*, 312−319.
(68) Tomita, K.; Petrykin, V.; Kobayashi, M.; Shiro, M.; Yoshimura, M.; Kakihana, M. *Angew. Chem. Int. Ed.* **2006**, *45*, 2378−2381.
(69) Morishima, Y.; Kobayashi, M.; Petrykin, V.; Yin, S.; Sato, T.; Kakihana, M.; Tomita, K. *J. Ceram. Soc. Jpn.* **2009**, *117*, 320−325.
(70) Kakihana, M.; Kobayashi, M.; Tomita, K.; Petrykin, V. *Bull. Chem. Soc. Jpn.* **2010**, *83*, 1285−1308.
(71) Kobayashi, M.; Petrykin, V.; Tomita, K.; Kakihana, M. *J. Cryst. Growth* **2011**, *337*, 30−37.
(72) Ohno, Y.; Tomita, K.; Komatsubara, Y.; Taniguchi, T.; Katsumata, K.; Matsushita, N.; Kogure, T.; Okada, K. *Cryst. Growth Des.* **2011**, *11*, 4831−4836.
(73) Nagase, T.; Ebina, T.; Iwasaki, T.; Hayashi, H.; Onodera, Y.; Chatterjee, M. *Chem. Lett.* **1999**, 911−912.
(74) Zheng, Y.; Shi, E.; Cui, S.; Li, W.; Hu, X. *J. Am. Ceram. Soc.* **2000**, *83*, 2634−2636.
(75) Zheng, Y.; Shi, E.; Cui, S.; Li, W.; Hu, X. *J. Mater. Sci. Lett.* **2000**, *19*, 1445−1448.
(76) Zheng, Y.; Shi, E.; Chen, Z.; Li, W.; Hu, X. *J. Mater. Chem.* **2001**, *11*, 1547−1551.
(77) Hu, W.; Li, L.; Li, G.; Tang, C.; Sun, L. *Cryst. Growth Des.* **2009**, *9*, 3676−3682.
(78) Kominami, H.; Ishii, Y.; Kohno, M.; Konishi, S.; Kera, Y.; Ohtani, B. *Catal. Lett.* **2003**, *91*, 41−47.
(79) Kobayashi, M.; Tomita, K.; Petrykin, V.; Yoshimura, M.; Kakihana, M. *J. Mater. Sci.* **2008**, *43*, 2158−2162.
(80) Sugimoto, T.; Zhou, X.; Muramatsu, A. *J. Colloid Interface Sci.* **2003**, *259*, 53−61.
(81) Taniguchi, T.; Watanabe, T.; Katsumata, K.; Okada, K.; Matsushita, N. *J. Phys. Chem. C* **2010**, *114*, 3769−3769.
(82) Tombácz, E.; Bica, D.; Hajdú, A.; Illés, E.; Majzik, A.; Vékás, L. *J. Phys.: Condens. Matter* **2008**, *20*, 204103.
(83) Sopyan, I.; Watanabe, M.; Murasawa, S.; Hashimoto, K.; Fujishima, A. *J. Photochem. Photobiol. A: Chem.* **1996**, *98*, 79−86.
(84) Yang, H. G.; Sun, C. H.; Qiao, S. Z.; Zou, J.; Gang, Liu.; Smith, S. C.; Cheng, H. M.; Lu, G. Q. *Nature* **2008**, *453*, 638−641.
(85) Yang, H. G.; Liu, G.; Qiao, S. Z.; Sun, C. H.; Jin, Y. G.; Smith, S. C.; Zou, J.; Cheng, H. M.; Lu, G. Q. *J. Am. Chem. Soc.* **2009**, *131*, 4078−4083.
(86) Amano, F.; Prieto-Mahaney, O.-O.; Terada, Y.; Yasumoto, Y.; Shibayama, T.; Ohtani, B. *Chem. Mater.* **2009**, *21*, 2601−2603.